Molecular dynamics simulation of O_2 adsorption on Ag(110) from first principles electronic structure calculations

Ivor Lončarić,[1,*] M. Alducin,[1,2,†] and J.I. Juaristi[3,1,2,‡]

[1] *Centro de Física de Materiales CFM/MPC (CSIC-UPV/EHU), Paseo Manuel de Lardizabal 5, 20018 Donostia-San Sebastián, Spain*
[2] *Donostia International Physics Center DIPC, P. Manuel de Lardizabal 4, 20018 San Sebastián, Spain*
[3] *Departamento de Física de Materiales, Facultad de Químicas, Universidad del País Vasco (UPV/EHU), Apartado 1072, 20080 San Sebastián, Spain*

Electronic Supplementary Information

I. CONVERGENCE STUDY

We perform convergence study of adsorption wells properties for several DFT calculation parameters. The properties we investigate are: adsorption energy (E_a), interatomic distance in the molecule ($r_{\mathrm{O-O}}$), vertical distance of the molecular center of mass to the surface ($Z_{\mathrm{O-Ag}}$), and spin polarisation (Sp). We define E_a as a difference between energy of the system with the molecule in the well and the energy of the system with molecule in the middle of vacuum region ($Z_{\mathrm{O-Ag}} \approx 9$ Å). This contrasts with the definition we used in the article, where zero potential energy was defined at $Z_{\mathrm{O-Ag}} = 6$ Å. Due to this, one may notice small (0.02 eV) difference in corresponding adsorption energies.

The convergence study provides insight in the precision one should expect from the calculations. It also helps to resolve the differences between previously published DFT results [1–9]. For most of the calculations presented here we use VASP code [10, 11] which includes a set of projector augmented wave method (PAW) pseudopotentials (PP) [12, 13]. For oxygen there are two types, soft PP with suggested plane-wave basis set cutoff of $E_{\mathrm{cut-off}} = 400$ eV and hard PP with suggested $E_{\mathrm{cut-off}} = 700$ eV. In addition to PP, we study the convergence in respect to the **k**-point mesh, cell size, and number of Ag layers. In all cases two uttermost surface layer atoms and O_2 atoms are relaxed until force on them was lower than 0.01 eV/Å. Additionally, for the sake of comparison we performed some calculations with QUANTUM ESPRESSO code [14] using GBRV [15] PP with $E_{\mathrm{cut-off}} = 680$ eV, which is above suggested $E_{\mathrm{cut-off}} = 540$ eV [15].

Our results are presented in Tables I-VI. In general, differences in $r_{\mathrm{O-O}}$, $Z_{\mathrm{O-Ag}}$, and Sp are very small regardless of the calculation parameters. Regarding the Sp we found that additional care has to be taken when obtaining the lowest energy state for the bridge wells. In practice we had to perform constrained spin calculation (we set spin to 2 Bohr magnetons μ_B) to obtain initial wavefunctions for the unconstrained calculation. If one proceeds with default VASP calculation in our experience results such as those denoted SBnsp and LBnsp in Table III are obtained. These results reproduce values obtained in Ref. [9].

Differences between calculation parameters are more pronounced for E_a. Regarding the **k**-point mesh, in most of the cases already 4×4 mesh suffices. The largest differences are due to the different PP. Harder VASP PP and GBRV PP generally reduce E_a in comparison to the softer VASP PP. This reduction is somewhat larger in the case of the hollow wells. Such results further increase the difficulty in explaining why the bridge wells are not observed in experiments. Unit cell parameters do not change results significantly.

TABLE I. Convergence study of adsorption wells properties in respect to the **k**-point sampling for soft VASP PP and 2×3 unit cell with 5 Ag layers.

site	slab	PP	**k**-point mesh	E_a(eV)	$r_{\mathrm{O-O}}$(Å)	$Z_{\mathrm{O-Ag}}$(Å)	$Sp(\mu_B)$
H110	$2 \times 3 \times 5$	soft	4×4	-0.38	1.45	1.03	0.00
H001	$2 \times 3 \times 5$	soft	4×4	-0.38	1.42	1.21	0.00
SB	$2 \times 3 \times 5$	soft	4×4	-0.36	1.31	2.16	1.24
LB	$2 \times 3 \times 5$	soft	4×4	-0.27	1.30	1.96	1.21
O_2	$2 \times 3 \times 5$	soft	4×4	-	1.24	9.65	-1.95
H110	$2 \times 3 \times 5$	soft	5×5	-0.42	1.46	1.00	0.00
H001	$2 \times 3 \times 5$	soft	5×5	-0.38	1.42	1.21	0.00
SB	$2 \times 3 \times 5$	soft	5×5	-0.35	1.31	2.15	1.20
LB	$2 \times 3 \times 5$	soft	5×5	-0.29	1.30	1.94	1.17
O_2	$2 \times 3 \times 5$	soft	5×5	-	1.24	9.65	-1.95
H110	$2 \times 3 \times 5$	soft	8×8	-0.38	1.46	1.01	0.00
H001	$2 \times 3 \times 5$	soft	8×8	-0.37	1.42	1.21	0.00
SB	$2 \times 3 \times 5$	soft	8×8	-0.34	1.31	2.16	1.26
LB	$2 \times 3 \times 5$	soft	8×8	-0.29	1.30	1.96	1.22
O_2	$2 \times 3 \times 5$	soft	8×8	-	1.24	9.65	-1.95
H110	$2 \times 3 \times 5$	soft	12×12	-0.39	1.46	1.00	0.00
H001	$2 \times 3 \times 5$	soft	12×12	-0.39	1.42	1.22	0.00
SB	$2 \times 3 \times 5$	soft	12×12	-0.35	1.31	2.16	1.25
LB	$2 \times 3 \times 5$	soft	12×12	-0.29	1.30	1.95	1.21
O_2	$2 \times 3 \times 5$	soft	12×12	-	1.24	9.65	1.95

TABLE II. Convergence study of adsorption wells properties in respect to the **k**-point sampling for hard VASP PP and 2×3 unit cell with 5 Ag layers.

site	slab	PP	**k**-point mesh	E_a(eV)	$r_{\mathrm{O-O}}$(Å)	$Z_{\mathrm{O-Ag}}$(Å)	$Sp(\mu_B)$
H110	$2 \times 3 \times 5$	hard	4×4	-0.26	1.45	1.00	0.00
H001	$2 \times 3 \times 5$	hard	4×4	-0.26	1.41	1.24	0.00
SB	$2 \times 3 \times 5$	hard	4×4	-0.29	1.30	2.18	1.28
LB	$2 \times 3 \times 5$	hard	4×4	-0.20	1.29	1.96	-1.24
O_2	$2 \times 3 \times 5$	hard	4×4	-	1.22	9.65	-1.96
H110	$2 \times 3 \times 5$	hard	5×5	-0.30	1.45	1.00	0.09
H001	$2 \times 3 \times 5$	hard	5×5	-0.27	1.41	1.24	0.00
SB	$2 \times 3 \times 5$	hard	5×5	-0.28	1.30	2.17	-1.24
LB	$2 \times 3 \times 5$	hard	5×5	-0.22	1.29	1.95	1.21
O_2	$2 \times 3 \times 5$	hard	5×5	-	1.22	9.65	-1.94
H110	$2 \times 3 \times 5$	hard	8×8	-0.26	1.45	1.01	0.02
H001	$2 \times 3 \times 5$	hard	8×8	-0.26	1.41	1.24	0.00
SB	$2 \times 3 \times 5$	hard	8×8	-0.28	1.30	2.18	-1.29
LB	$2 \times 3 \times 5$	hard	8×8	-0.22	1.29	1.94	1.24
O_2	$2 \times 3 \times 5$	hard	8×8	-	1.22	9.65	-1.94

TABLE III. Convergence study of adsorption wells properties in respect to the **k**-point sampling for soft VASP PP and 3×4 unit cell with 5 Ag layers.

site	slab	PP	**k**-point mesh	E_a(eV)	$r_{\mathrm{O-O}}$(Å)	$Z_{\mathrm{O-Ag}}$(Å)	$Sp(\mu_B)$
H110	$3 \times 4 \times 5$	soft	4×4	-0.40	1.46	1.04	0.00
H001	$3 \times 4 \times 5$	soft	4×4	-0.38	1.42	1.26	0.00
SB	$3 \times 4 \times 5$	soft	4×4	-0.35	1.31	2.20	1.25
LB	$3 \times 4 \times 5$	soft	4×4	-0.29	1.30	2.01	1.25
O_2	$3 \times 4 \times 5$	soft	4×4	-	1.24	9.09	-1.93
H110	$3 \times 4 \times 5$	soft	5×5	-0.39	1.46	1.05	0.00
H001	$3 \times 4 \times 5$	soft	5×5	-0.38	1.42	1.26	0.00
SB	$3 \times 4 \times 5$	soft	5×5	-0.36	1.31	2.20	1.19
LB	$3 \times 4 \times 5$	soft	5×5	-0.30	1.30	2.01	1.24
O_2	$3 \times 4 \times 5$	soft	5×5	-	1.24	9.10	-1.93
SBnsp	$3 \times 4 \times 5$	soft	5×5	-0.10	1.34	2.06	-0.07
LBnsp	$3 \times 4 \times 5$	soft	5×5	-0.11	1.33	1.84	0.01
H110	$3 \times 4 \times 5$	soft	8×8	-0.41	1.46	1.04	0.00
H001	$3 \times 4 \times 5$	soft	8×8	-0.38	1.42	1.25	0.00
SB	$3 \times 4 \times 5$	soft	8×8	-0.36	1.31	2.20	1.21
LB	$3 \times 4 \times 5$	soft	8×8	-0.30	1.30	2.01	1.23
O_2	$3 \times 4 \times 5$	soft	8×8	-	1.24	9.10	-1.93

TABLE IV. Convergence study of adsorption wells properties in respect to the **k**-point sampling for hard VASP PP and 2×3 unit cell with 5 Ag layers.

site	slab	PP	**k**-point mesh	E_a(eV)	$r_{\mathrm{O-O}}$(Å)	$Z_{\mathrm{O-Ag}}$(Å)	$Sp(\mu_B)$
H110	$3 \times 4 \times 5$	hard	4×4	-0.29	1.45	1.00	0.00
H001	$3 \times 4 \times 5$	hard	4×4	-0.27	1.41	1.25	0.00
SB	$3 \times 4 \times 5$	hard	4×4	-0.28	1.30	2.18	-1.28
LB	$3 \times 4 \times 5$	hard	4×4	-0.22	1.29	2.00	-1.27
O_2	$3 \times 4 \times 5$	hard	4×4	-	1.23	9.10	1.95
H110	$3 \times 4 \times 5$	hard	5×5	-0.28	1.45	1.01	0.00
H001	$3 \times 4 \times 5$	hard	5×5	-0.28	1.41	1.25	0.00
SB	$3 \times 4 \times 5$	hard	5×5	-0.29	1.30	2.17	-1.23
LB	$3 \times 4 \times 5$	hard	5×5	-0.24	1.29	2.01	-1.31
O_2	$3 \times 4 \times 5$	hard	5×5		-1.23	9.10	1.95
H110	$3 \times 4 \times 5$	hard	8×8	-0.30	1.45	1.01	0.00
H001	$3 \times 4 \times 5$	hard	8×8	-0.28	1.41	1.25	0.00
SB	$3 \times 4 \times 5$	hard	8×8	-0.29	1.30	2.17	-1.24
LB	$3 \times 4 \times 5$	hard	8×8	-0.23	1.29	1.96	-1.26
O_2	$3 \times 4 \times 5$	hard	8×8		1.23	9.10	1.95

TABLE V. Convergence study of adsorption wells properties in respect to the **k**-point sampling for soft VASP PP and 2×3 unit cell with 10 Ag layers.

site	slab	PP	**k**-point mesh	E_a(eV)	$r_{\mathrm{O-O}}$(Å)	$Z_{\mathrm{O-Ag}}$(Å)	$Sp(\mu_B)$
H110	$2 \times 3 \times 10$	soft	4×4	-0.35	1.45	1.05	0.22
H001	$2 \times 3 \times 10$	soft	4×4	-0.38	1.42	1.24	0.00
SB	$2 \times 3 \times 10$	soft	4×4	-0.38	1.31	2.14	1.23
LB	$2 \times 3 \times 10$	soft	4×4	-0.31	1.30	1.96	1.24
O_2	$2 \times 3 \times 10$	soft	4×4	-	1.24	9.09	-1.95
H110	$2 \times 3 \times 10$	soft	5×5	-0.42	1.45	1.05	0.01
H001	$2 \times 3 \times 10$	soft	5×5	-0.42	1.42	1.24	0.00
SB	$2 \times 3 \times 10$	soft	5×5	-0.37	1.31	2.14	1.21
LB	$2 \times 3 \times 10$	soft	5×5	-0.33	1.30	1.95	1.22
O_2	$2 \times 3 \times 10$	soft	5×5	-	1.24	9.10	-1.95
H110	$2 \times 3 \times 10$	soft	8×8	-0.42	1.45	1.05	0.00
H001	$2 \times 3 \times 10$	soft	8×8	-0.43	1.42	1.24	0.00
SB	$2 \times 3 \times 10$	soft	8×8	-0.38	1.31	2.14	1.19
LB	$2 \times 3 \times 10$	soft	8×8	-0.33	1.30	1.95	1.23
O_2	$2 \times 3 \times 10$	soft	8×8	-	1.24	9.13	-1.95

TABLE VI. Convergence study of adsorption wells properties in respect to the **k**-point sampling for GBRV [15] PP and 2×3 unit cell with 5 Ag layers calculated with QUANTUM ESPRESSO code [14].

site	slab	PP	**k**-point mesh	E_a(eV)	$r_{\mathrm{O-O}}$(Å)	$Z_{\mathrm{O-Ag}}$(Å)	$Sp(\mu_B)$
H110	$2 \times 3 \times 5$	GBRV	4×4	-0.22	1.45	1.02	0.00
H001	$2 \times 3 \times 5$	GBRV	4×4	-0.21	1.42	1.21	0.00
SB	$2 \times 3 \times 5$	GBRV	4×4	-0.27	1.30	2.18	1.30
LB	$2 \times 3 \times 5$	GBRV	4×4	-0.20	1.29	2.01	1.32
O_2	$2 \times 3 \times 5$	GBRV	4×4	-	1.23	9.00	1.96
H110	$2 \times 3 \times 5$	GBRV	5×5	-0.26	1.45	1.00	0.00
H001	$2 \times 3 \times 5$	GBRV	5×5	-0.26	1.42	1.22	0.00
SB	$2 \times 3 \times 5$	GBRV	5×5	-0.27	1.30	2.18	1.30
LB	$2 \times 3 \times 5$	GBRV	5×5	-0.22	1.29	2.01	1.30
O_2	$2 \times 3 \times 5$	GBRV	5×5	-	1.23	9.00	1.96
H110	$2 \times 3 \times 5$	GBRV	8×8	-0.23	1.45	1.00	0.00
H001	$2 \times 3 \times 5$	GBRV	8×8	-0.23	1.42	1.22	0.00
SB	$2 \times 3 \times 5$	GBRV	8×8	-0.26	1.30	2.18	1.31
LB	$2 \times 3 \times 5$	GBRV	8×8	-0.21	1.29	2.01	1.31
O_2	$2 \times 3 \times 5$	GBRV	8×8	-	1.23	9.00	1.96
H110	$2 \times 3 \times 5$	GBRV	12×12	-0.24	1.45	1.00	0.00
H001	$2 \times 3 \times 5$	GBRV	12×12	-0.23	1.42	1.22	0.00
SB	$2 \times 3 \times 5$	GBRV	12×12	-0.26	1.30	2.18	1.30
LB	$2 \times 3 \times 5$	GBRV	12×12	-0.21	1.29	2.01	1.31
O_2	$2 \times 3 \times 5$	GBRV	12×12	-	1.23	9.00	1.96

II. BARRIERS BETWEEN THE ADSORPTION WELLS

Figs. 1-6 show results of climbing image nudged elastic band (CI-NEB) method for finding transition barriers between the four wells. In all cases we use 5 images between initial and final state. The results from the 6D PES [8] are obtained using the *Atomic Simulation Environment* (ASE) [16] with force convergence criteria set to 0.005 eV/Å. The results in which the two uppermost silver layers are allowed to relax are obtained using the VASP code extended with *Transition State Tools for VASP* code [17–20]. Force convergence criteria is set to 0.05 eV/Å. All other DFT parameters are the same as those used in the construction of 6D PES [8].

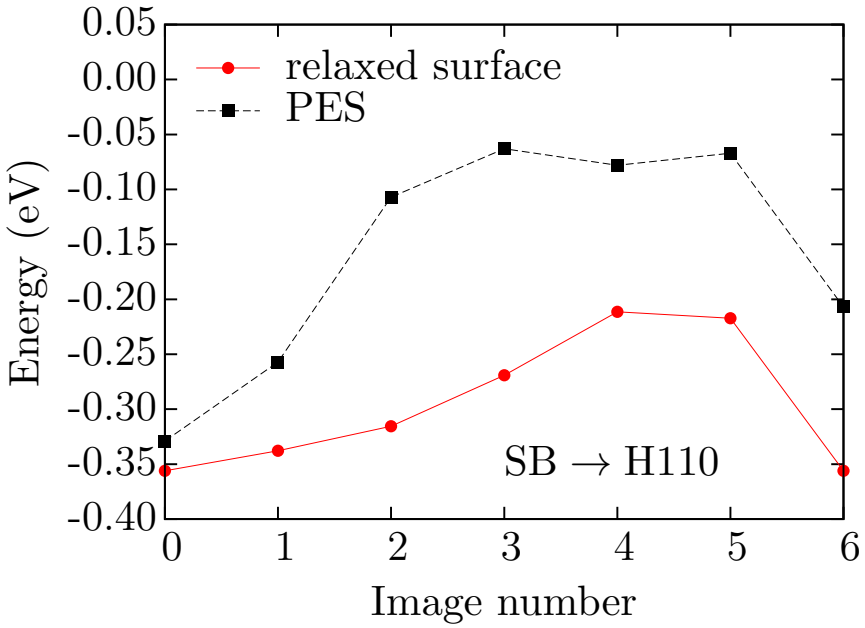

FIG. 1. Climbing image nudged elastic band method results for transition from the SB well to the H110 well. Black line represent results for frozen surface (energy and forces are given by PES). Red line represents moving surface results (energy and forces from VASP).

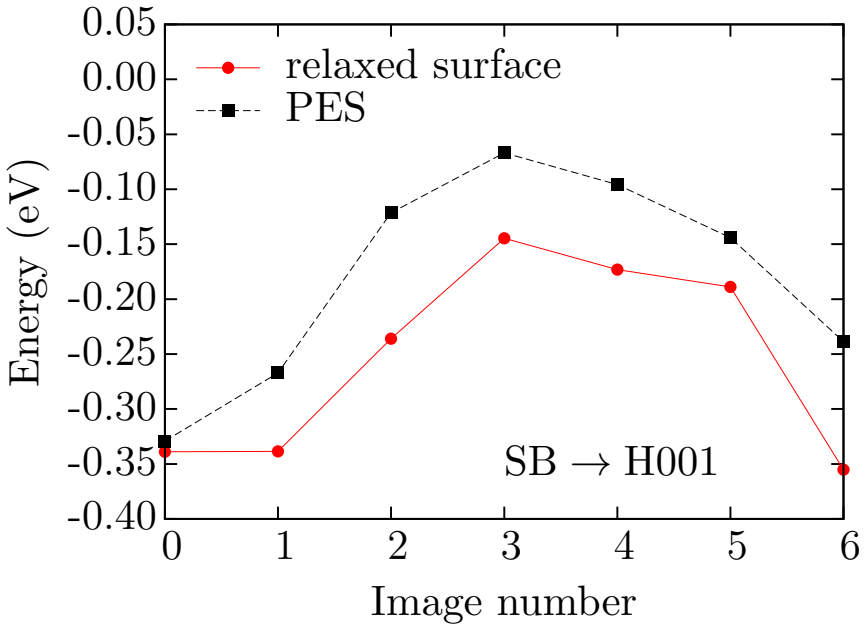

FIG. 2. Same as Fig. 1 for transition from the SB well to the H001 well.

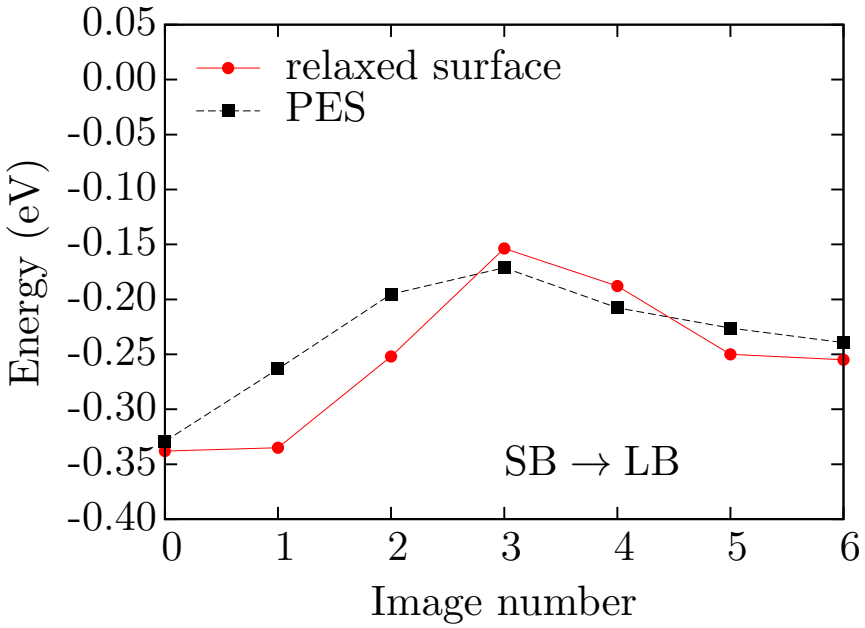

FIG. 3. Same as Fig. 1 for transition from the SB well to the LB well.

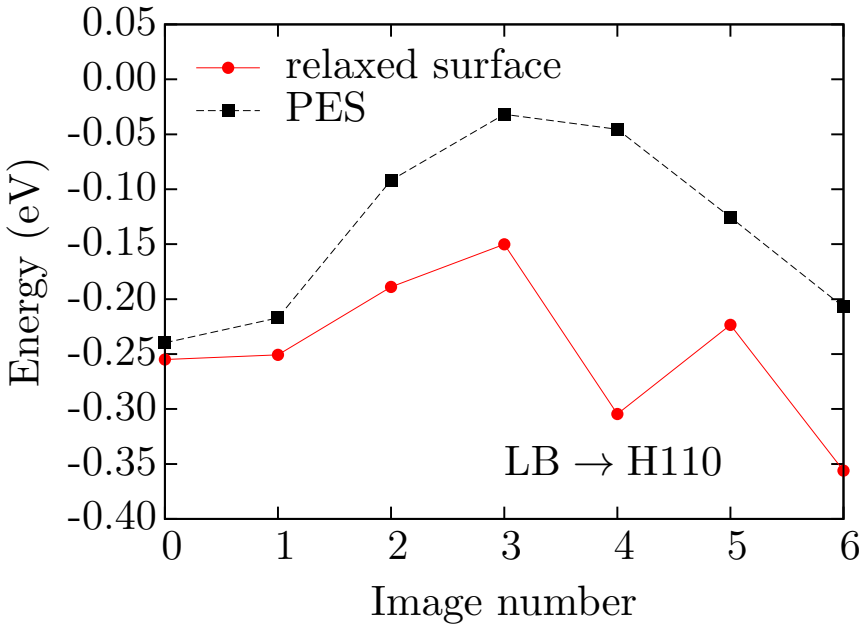

FIG. 4. Same as Fig. 1 for transition from the LB well to the H110 well.

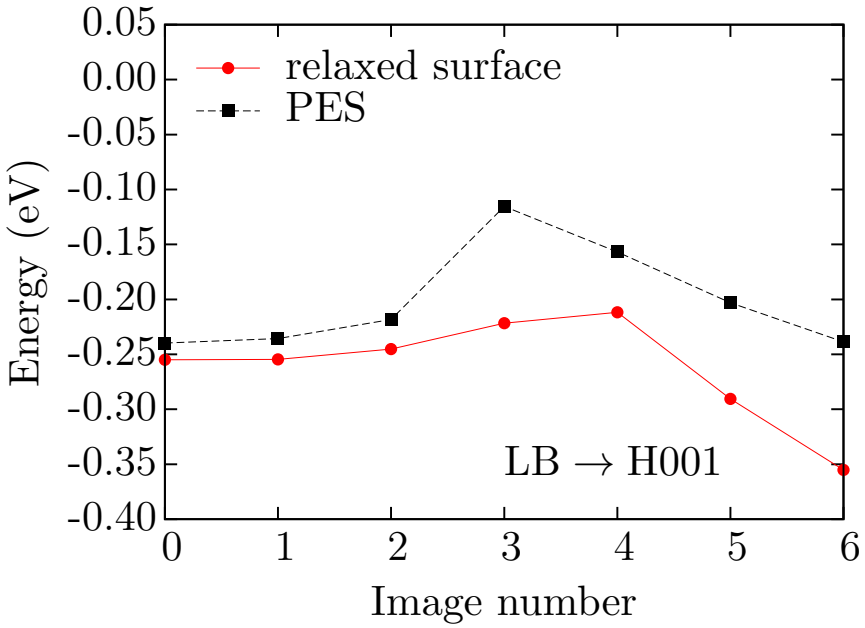

FIG. 5. Same as Fig. 1 for transition from the LB well to the H001 well.

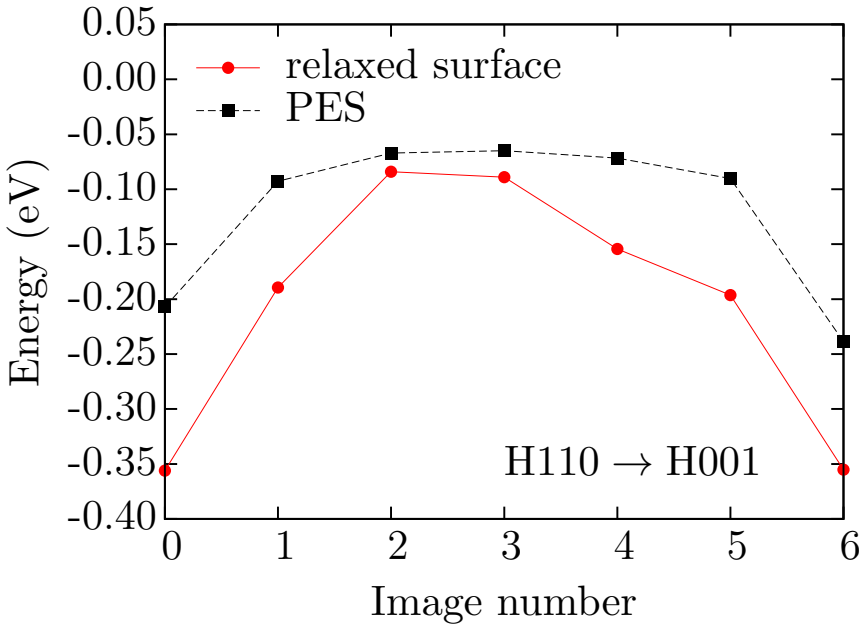

FIG. 6. Same as Fig. 1 for transition from the H110 well to the H001 well.

* ivor.loncaric@gmail.com
† wapalocm@ehu.es
‡ josebainaki.juaristi@ehu.es

[1] P. Gravil, J. White, and D. Bird, Surf. Sci. **352-354**, 248 (1996).
[2] P. A. Gravil, D. M. Bird, and J. A. White, Phys. Rev. Lett. **77**, 3933 (1996).
[3] D. Bird and P. Gravil, Surf. Sci. **377-379**, 555 (1997).
[4] M. Alducin, D. Sánchez-Portal, A. Arnau, and N. Lorente, Phys. Rev. Lett. **104**, 136101 (2010).
[5] S. Monturet, M. Alducin, and N. Lorente, Phys. Rev. B **82**, 085447 (2010).
[6] F. Olsson, N. Lorente, and M. Persson, Surf. Sci. **522**, L27 (2003).
[7] S. Roy, V. Mujica, and M. A. Ratner, J. Chem. Phys. **139**, 074702 (2013).
[8] I. Lončarić, M. Alducin, and J. I. Juaristi, Phys. Chem. Chem. Phys. **17**, 9436 (2015).
[9] T. B. Rawal, S. Hong, A. Pulkkinen, M. Alatalo, and T. S. Rahman, Phys. Rev. B **92**, 035444 (2015).
[10] G. Kresse and J. Furthmüller, Comput. Mater. Sci. **6**, 15 (1996).
[11] G. Kresse and J. Furthmüller, Phys. Rev. B **54**, 11169 (1996).
[12] P. E. Blöchl, Phys. Rev. B **50**, 17953 (1994).
[13] G. Kresse and D. Joubert, Phys. Rev. B **59**, 1758 (1999).
[14] P. Giannozzi, S. Baroni, N. Bonini, M. Calandra, R. Car, C. Cavazzoni, D. Ceresoli, G. L. Chiarotti, M. Cococcioni, I. Dabo, A. Dal Corso, S. de Gironcoli, S. Fabris, G. Fratesi, R. Gebauer, U. Gerstmann, C. Gougoussis, A. Kokalj, M. Lazzeri, L. Martin-Samos, N. Marzari, F. Mauri, R. Mazzarello, S. Paolini, A. Pasquarello, L. Paulatto, C. Sbraccia, S. Scandolo, G. Sclauzero, A. P. Seitsonen, A. Smogunov, P. Umari, and R. M. Wentzcovitch, J. Phys.: Condens. Matter **21**, 395502 (19pp) (2009).
[15] K. F. Garrity, J. W. Bennett, K. M. Rabe, and D. Vanderbilt, Comput. Mater. Sci. **81**, 446 (2014).
[16] S. R. Bahn and K. W. Jacobsen, Comput. Sci. Eng. **4**, 56 (2002).
[17] G. Henkelman, B. P. Uberuaga, and H. Jónsson, J. Chem. Phys. **113**, 9901 (2000).
[18] G. Henkelman and H. Jónsson, J. Chem. Phys. **113**, 9978 (2000).
[19] D. Sheppard, R. Terrell, and G. Henkelman, J. Chem. Phys. **128**, 134106 (2008), 10.1063/1.2841941.
[20] D. Sheppard and G. Henkelman, J. Comput. Chem. **32**, 1769 (2011).